

## ONE METHOD OF PRODUCING A HIGH-TEMPERATURE DENSE PLASMA

V. Ya. Ternovoi,<sup>1</sup> K. V. Khishchenko,<sup>2</sup> and A. A. Charakhch'yan<sup>3</sup>

UDC 533.9.03

*This paper considers the interaction between an absolutely rigid wall or a steel plate and the rarefaction wave arising in solid deuterium when a 30–150 GPa shock wave arrives at the free surface. It is shown that, in the entropy trace near the wall or interface with the plate, a high-temperature plasma arises, in which a thermonuclear fusion is possible, at least, for shock-wave pressures above 70 GPa. The dimension of the plasma region and the time of its establishment are proportional to the distance between the free surface and the wall. Estimates of the proportionality coefficients are given. It is noted that, in this case, unlike in other methods of high-temperature plasma generation, the time of existence of the plasma may not depend on the sound velocity in it. It is shown that, by using a conical solid-state target with an exit hole, the shock-wave pressure in solid deuterium can be increased from 10 to 100 GPa.*

**Key words:** shock wave, a rarefaction wave, entropy trace, high-temperature plasma, solid deuterium, thermonuclear fusion, conical target.

**Introduction.** In many papers, the rarefaction wave arising from strong shock waves which arrive at the free surface of a solid body has been studied from a viewpoint of the possibility of determining the temperature and entropy in the shock wave (see, for example, [1]). The effect of formation of a high-temperature plasma upon the interaction of such a rarefaction wave with a plate was found experimentally in [2] for shock waves in lead. The possibility of considerable heating of a small part of the material near the wall was noted even in 1947 by Zel'dovich and Stanyukovich in an analytical study of the initial stage of interaction of a rarefaction wave in an ideal gas with an absolutely solid wall [3].

In the present work, we solve the problem of the interaction of a rarefaction wave with an absolutely solid wall after the arrival of a shock wave on the free boundary of deuterium ice. The same problem is examined with a steel plate instead of an absolutely solid wall. The equations of state for deuterium  $p = p(\rho, T)$  and  $\varepsilon = \varepsilon(\rho, T)$  ( $p$  is the pressure,  $\rho$  is the density,  $T$  is the temperature, and  $\varepsilon$  is the specific internal energy) were obtained with use of the equations of state for hydrogen  $p = p_H(\rho, T)$  and  $\varepsilon = \varepsilon_H(\rho, T)$  [4] by the formulas

$$p(\rho, T) = p_H(\rho/2, T), \quad \varepsilon(\rho, T) = \varepsilon_H(\rho/2, T)/2.$$

The equations of state obtained in this way describe experimental data [5] on the shock compressibility of solid deuterium, and the region of a completely ionized rarefied plasma is described by the corresponding ideal gas equations of state. The equations of state for steel were constructed according to [6].

The introduction of a strong shock wave into a light medium involves difficulties described, for example, in [7]. In particular, on reaching the interface with solid deuterium, a 250 GPa shock wave in steel becomes a shock wave with a pressure of approximately 10 GPa. At present, in the world there is, apparently, only one facility (at the Sandia National Laboratories in the United States) which produces shock waves with a pressure up to 100 GPa in solid deuterium by means of flat impactors [5]. In Sec. 3 of the present paper, we study the possibility of shock-wave amplification in solid deuterium by using conical targets.

---

<sup>1</sup>Institute of Problems of Chemical Physics, Russian Academy of Sciences, Chernogolovka 142432. <sup>2</sup>Joint Institute of High Temperatures, Russian Academy of Sciences, Moscow 125412. <sup>3</sup>Dorodnitsyn Computer Center of the Russian Academy of Sciences, 119333 Moscow; chara@ccas.ru. Translated from *Prikladnaya Mekhanika i Tekhnicheskaya Fizika*, Vol. 50, No. 3, pp. 15–24, May–June, 2009. Original article submitted September 20, 2007; revision submitted February 6, 2008.

**1. Interaction of a Rarefaction Wave with an Absolutely Solid Wall.** For the one-dimensional equations of hydrodynamics

$$\frac{d\rho}{dt} = -\rho \operatorname{div} u, \quad \frac{du}{dt} = -\nabla p, \quad \rho \frac{d(\varepsilon + u^2/2)}{dt} = -\operatorname{div} pu \quad (1)$$

( $t$  is time,  $u$  is the velocity,  $\operatorname{div} u = \partial u / \partial x$ ,  $\nabla p = \partial p / \partial x$ ;  $x$  is the spatial coordinate, and  $d/dt = \partial / \partial t + u \partial / \partial x$  is the Lagrangian time derivative), the following problem is studied. A motionless material at a pressure  $p_a = 0.1$  MPa of normal solid-state density [the equations of state for  $p = p(\rho, T)$  and  $\varepsilon = \varepsilon(\rho, T)$ ] occupies the half-space  $x \geq 0$  (right). A shock wave with a pressure behind the front  $p_s$ , far exceeding the yield point, moves from right to left in the material. The values of the other functions behind the shock front, in particular, the velocities  $u_s < 0$ , are determined from the conservation laws at the wave front and the equations of state. At the point  $x = 0$ , the shock wave reaches the free boundary at a pressure  $p_a$ . At the point  $x = -h$ ,  $h > 0$ , there is an absolutely solid wall.

Before the arrival of the free boundary at the wall, the solution of the problem is self-similar and consists of a centered rarefaction wave and regions of constant flow (see, for example, [1]). The required functions depend on the variable  $\xi = x/t$ , where the time  $t$  is reckoned from the moment of shock-wave arrival at the free boundary. In the centered rarefaction wave  $\xi = u + c$ , where the sound velocity  $c = \sqrt{(\partial p / \partial \rho)_S}$  is defined by derivatives of the equations of state for ( $S$  is the entropy). The equation of the isentrope

$$d\varepsilon + p dv = 0$$

( $v = \rho^{-1}$  is the specific volume) and the equation of state are integrated, for example, in the plane  $(\rho, T)$  from the postshock pressure to the value  $p_a$ . The velocity is defined by the formula

$$u = u_s + \int_{p_s}^p \frac{dp}{\rho c},$$

where integration is performed along the isentrope. As a result, all required functions, in particular,  $p = p_r(\xi)$ , are defined on the interval  $u_a + c_a = \xi_a \leq \xi \leq \xi_s = u_s + c_s$ , where  $u_a$  and  $c_a$  are the velocity of the free boundary and the sound velocity on it. Over the entire region, the solution has the form

$$p(x, t) = \begin{cases} p_s, & \xi \geq \xi_s, \\ p_r(\xi), & \xi_a \leq \xi \leq \xi_s, \\ p_a, & u_a \leq \xi \leq \xi_a; \end{cases}$$

for the other functions, the solution is similar.

At the time  $t_* = -h/u_a$ , the free boundary approaches the wall. The corresponding functions, for example  $p(x, t_*)$ , are initial data for the subsequent non-self-similar solution of the problem. Because the velocity  $u_a$  does not depend on the quantity  $h$ , these initial data for any  $h$  depend on the variable  $\eta = x/h$ . Because the equations of hydrodynamics are not changed by multiplication of the quantities  $x$  and  $t$  by the same constant, the solution of the problem for any value of  $h$  depends on the variables  $\eta$  and  $\tau = t[x]/h[t]$ , where  $t$  is the time reckoned from the moment of arrival of the free boundary at the wall, and  $[x]$  and  $[t]$  are the chosen measurement units (in the present work,  $[x] = 1$  mm and  $[t] = 1$   $\mu$ sec).

The problem is solved numerically using Godunov method of the first order of accuracy on fairly fine Lagrangian grids which are uniform along the coordinate  $x$  at the initial time. The calculation results for deuterium ice (initial density  $\rho_0 \approx 0.175$  g/cm<sup>3</sup> and initial temperature  $T_0 = 4$  K), and a shock pressure  $p_s = 70$  GPa are shown in Fig. 1. In Fig. 1a and b, it is evident that, with time, the solution becomes a shock wave propagating from the wall. The postshock values of the functions coincide with high accuracy with the values obtained by calculation of the reflection of a shock wave with a pressure  $p_s$  from an absolutely solid wall by the repeated shock-compression adiabat. This result can be predicted because, in the variables  $(x, t)$ , the solution of the problem for  $h \rightarrow 0$  should tend to the solution for  $h = 0$ , which is the reflected shock wave.

After the formation of the reflected wave, a motionless entropy trace with pressure behind the reflected-wave front  $p_{ss}$  remains near the wall. With decreasing distance to the wall, the density in the trace decreases considerably (Fig. 1c), but exceeds the density on the free boundary of the rarefaction wave by a factor of 200–300. In Fig. 1c, it is evident that the temperature, in contrast, considerably increases in approaching the wall, especially, in a

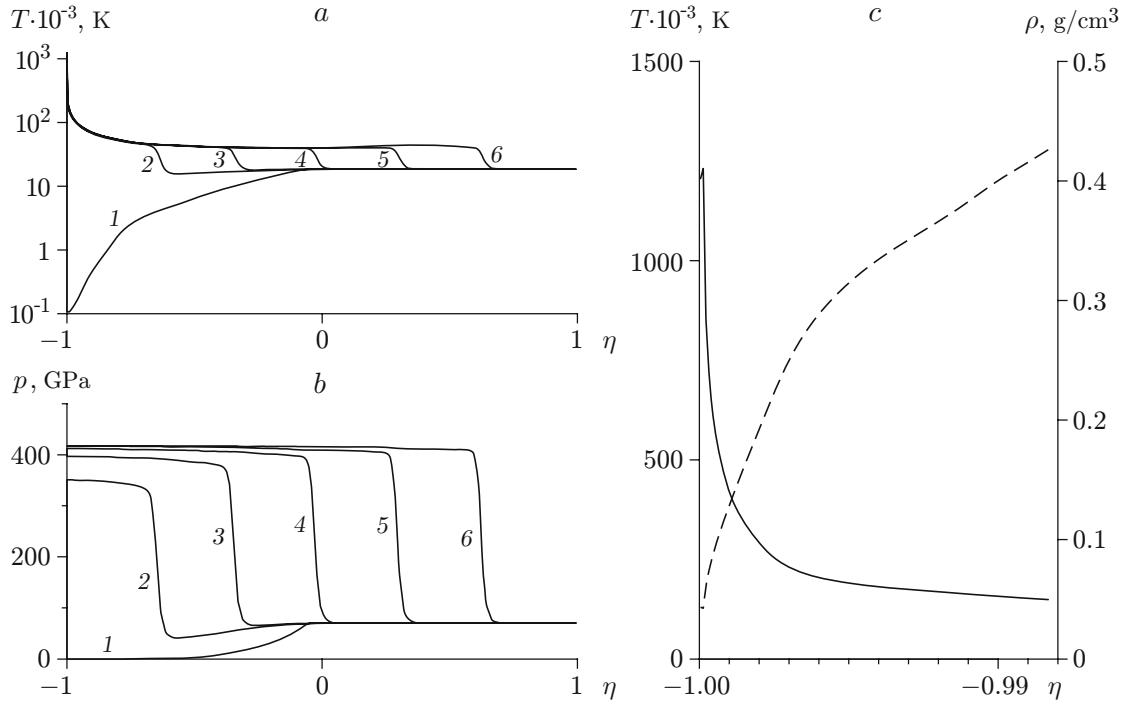


Fig. 1. Results of solution of the equations of hydrodynamics in the problem with an absolutely solid wall at  $p_s = 70$  GPa: (a, b) the temperature and pressure at various times  $\tau = 0$  (1), 1 (2), 2 (3), 3 (4), 4 (5), and 5 (6); (c) temperature profiles (solid curve) and density profiles (dashed curve) in the entropy trace near the wall.

narrow layer approximately  $10^{-3}h$  thick. For the chosen pressure  $p_s$ , the temperature at the reflected wave front is  $T_{ss} \approx 4 \cdot 10^4$  K, and wall temperature  $T_b \approx 12 \cdot 10^5$  K.

For the chosen density  $\rho$ , the temperature  $T$  in the entropy trace is determined from the equations of state for  $p_{ss} = p(\rho, T)$ , where the pressure  $p_{ss}$  is determined from the pressure  $p_s$  and repeated shock-compression adiabat. The results of this thermodynamic calculation are shown in Figs. 2 and 3. Figure 2 gives the dependence  $T(p_s)$  ( $30 \leq p_s \leq 100$  GPa) for density values  $\rho = \rho_0$ ,  $\rho = \rho_0/2$ , and  $\rho = \rho_c = 0.06$   $\text{g/cm}^3$ , which correspond to the solid and liquid states. In this case, the value  $\rho = \rho_c = 0.06$   $\text{g/cm}^3$  is approximately twice the hydrogen density at the critical point and corresponds to a particle concentration approximately equal to  $2 \cdot 10^{22}$   $\text{cm}^{-3}$ . The calculations were performed for values of  $p_s$  which are multiples of 10 GPa. In Fig. 2, it is evident that the temperature increases linearly with increasing  $p_s$ .

The high temperature values are due to two factors. First, as follows from Fig. 2, the pressure in the reflected wave is almost six times higher than the pressure in the incident wave. Second, even for density values characteristic of the solid and liquid states, the corresponding isobars of deuterium have the form of ideal gas isobars  $\rho T = \text{const}$ , which admit a considerable increase in temperature with decreasing density (see Fig. 3).

**2. Interaction of a Rarefaction Wave with a Plate.** We consider the problem in which, instead of an absolutely solid wall at  $x = -h$ , there is one more motionless material (plate) of constant density at a pressure  $p_a$  which occupies the half-space  $x \leq -h$ . As in the case of an absolutely solid wall, the solution of this problem for any  $h > 0$  depends on the variables  $\eta = x/h$  and  $\tau = t[x]/h[t]$ , where the value  $t = 0$  corresponds to the moment when the free boundary of the rarefaction wave arrives at the point  $x = -h$ . At  $h = 0$ , the solution of the problem is the reflected shock wave or the centered rarefaction wave and the shock wave in the plate, whose parameters and the velocity of the interface are found by solving the corresponding problem of discontinuity decay. The passage to the limit a  $h \rightarrow 0$  is due to the presence of the entropy trace near the interface, whose dimensions and time of formation also tend to zero as  $h \rightarrow 0$ .

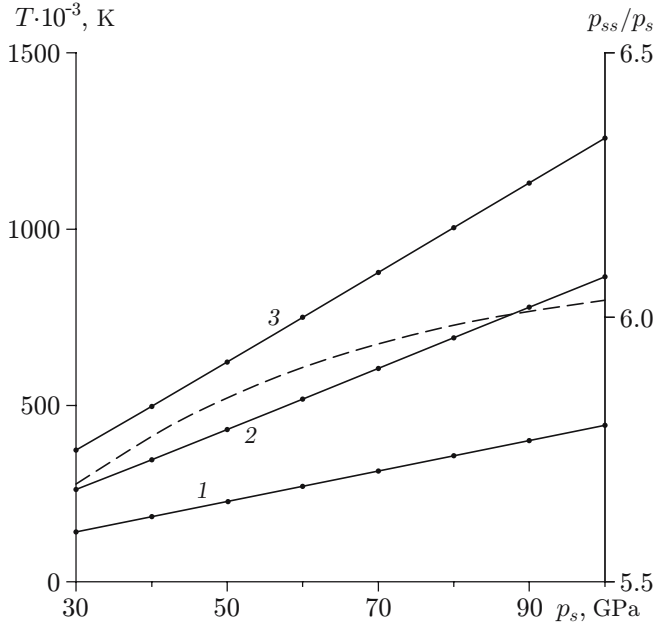


Fig. 2

Fig. 2. Temperature (solid curves) and pressure ratios  $p_{ss}/p_s$  in the reflected and incident waves (dashed curve) versus pressure  $p_s$ : curve 1 and 2 refer to  $\rho = \rho_0$  and  $\rho_0/2$ , respectively, and curve 3 refers to  $\rho_c = 0.06 \text{ g/cm}^3$ .

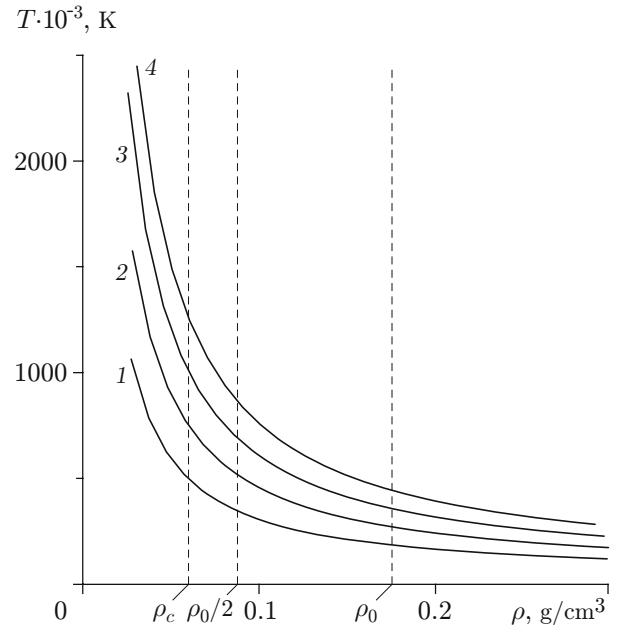


Fig. 3

Fig. 3. Isobars (solid curves) and isochores (dashed curves) in the entropy trace in deuterium for  $p_s = 40$  (1), 60 (2), 80 (3), and 100 GPa (4).

In the case of a steel plate, the problem was solved for the shock waves in solid deuterium considered above. In comparison with the case of an absolutely solid wall, the reflected shock-wave pressure  $p_{ss}$  decreases. For example, for a shock wave with a pressure  $p_s = 70 \text{ GPa}$  in the case of an absolutely solid wall,  $p_{ss} \approx 417 \text{ GPa}$ , and in the case of a steel plate,  $p_{ss} \approx 304 \text{ GPa}$ . Accordingly, this leads to a decrease the temperature in the entropy trace, which, along with the density, is described by the isobar  $p(\rho, T) = p_{ss}$ . As it might be expected, a narrow region of a high-temperature deuterium plasma in this problem occurs near the moving interface with steel (Fig. 4). This region is formed simultaneously with the reflected shock wave and moves together with interface at the constant velocity determined in the discontinuity decay problem. In Fig. 4, it is evident that, as  $\tau \rightarrow \infty$ , the velocity of the interface  $u_b(\tau)$  and the deuterium temperature on the boundary  $T_b(\tau)$  tends monotonically to the limiting values.

Figure 5 gives steady-state temperature profiles for the above cases of a shock wave with a pressure  $p_s = 70 \text{ GPa}$  and a shock wave with a pressure  $p_s = 100 \text{ GPa}$  and a steel plate. In the latter case, the pressure in the reflected wave is  $p_{ss} \approx 432 \text{ GPa}$ , which is only slightly higher than the value of  $p_{ss}$  for a shock wave with a pressure  $p_s = 70 \text{ GPa}$  and an absolutely solid wall. Despite the closeness of the values of  $p_{ss}$ , the deuterium temperature at the interface for a shock wave with a pressure  $p_s = 100 \text{ GPa}$  and a steel plate far exceeds the corresponding temperature for a shock wave with a pressure  $p_s = 70 \text{ GPa}$  and an absolutely solid wall, which is due to the lower density at the interface in the first case.

After the completion of the formation of the reflected shock wave, the deuterium temperature at the interface with the plate, similarly to the temperature on the absolutely solid wall in the problem from Sec. 1, reaches the maximum value  $T_{\max}$  and the density the minimum value  $\rho_{\min}$ . These values and the temperature values for  $\rho = \rho_c$  for two shock waves ( $p_s = 100$  and  $150 \text{ GPa}$ ) and two problems are given in Table 1. In all cases, the particle concentration at the interface is of the order of  $10^{22} \text{ cm}^{-3}$ . In transition from an absolutely solid wall to a steel plate, the temperature at the interface decreases not so much as the temperature at a fixed density linearly dependent on the reflected-wave pressure  $p_{ss}$ .

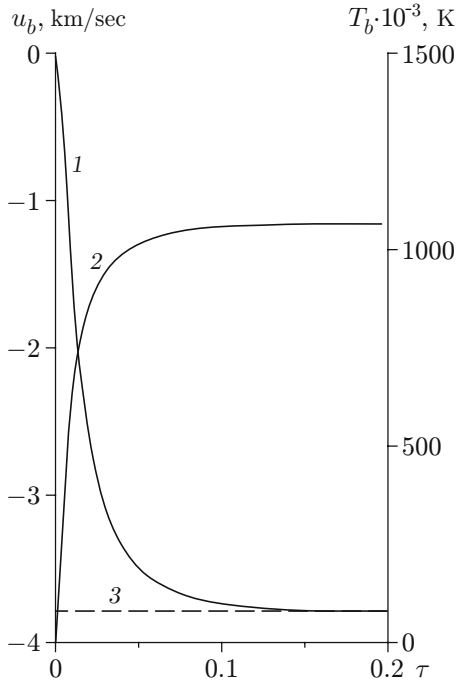


Fig. 4

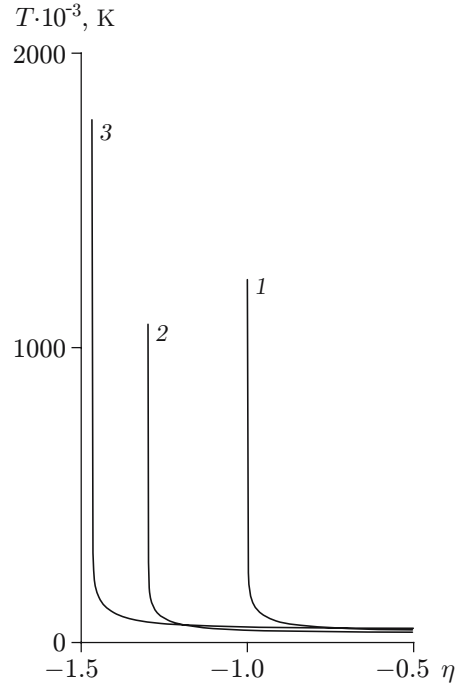


Fig. 5

Fig. 4. Velocity of the interface between deuterium and a steel plate  $u_b$  (1), deuterium temperature at the interface  $T_b$  (2) at  $p_s = 70$  GPa, and velocity  $u_b$  in the discontinuity decay problem (3) versus dimensionless time  $\tau$ .

Fig. 5. Steady-state temperature profiles in the entropy trace in the case of an absolutely solid wall at  $p_s = 70$  GPa (1) and in the case of a steel plate at  $p_s = 70$  (2) and 100 GPa (3).

TABLE 1

Values of Physical Parameters in Problems with an Absolutely Solid Wall and a Steel Plate

| Type of obstacle | $p_s$ , GPa | $\rho_{\min}$ , g/cm <sup>3</sup> | $T_{\max} \cdot 10^{-6}$ , K | $T_c \cdot 10^{-6}$ , K | $\tau_0$ | $\xi_{01}$          | $\xi_{02}$        |
|------------------|-------------|-----------------------------------|------------------------------|-------------------------|----------|---------------------|-------------------|
| Wall             | 100         | 0.040                             | 2.0                          | 1.3                     | 0.030    | $1.5 \cdot 10^{-4}$ | $4 \cdot 10^{-4}$ |
| Plate            | 100         | 0.030                             | 1.8                          | 0.9                     | 0.030    | $1.8 \cdot 10^{-4}$ | $4 \cdot 10^{-4}$ |
| Wall             | 150         | 0.030                             | 3.7                          | 1.9                     | 0.025    | $1.4 \cdot 10^{-4}$ | $10^{-3}$         |
| Plate            | 150         | 0.025                             | 3.2                          | 1.3                     | 0.020    | $1.7 \cdot 10^{-4}$ | $10^{-3}$         |

The dimensionless time of establishment of a high-temperature plasma  $\tau_0$  is given by the formula

$$T_b(\tau_0) = 0.9T_{\max}, \quad (2)$$

and the establishment time by the formula

$$\Delta t = \tau_0 h. \quad (3)$$

Let  $\eta_b(\tau)$  be the coordinate of the interface. Introducing the variable  $\xi = \eta - \eta_b(\tau)$ , we consider the steady-state deuterium temperature profile as a function  $T(\xi)$ ,  $\xi \geq 0$ . The function  $T(\xi)$  decreases monotonically:  $T(0) = T_{\max}$ . The width of the high-temperature plasma region  $\xi_0$  can be determined by two different methods:

$$T(\xi_{01}) = 0.9T_{\max}, \quad T(\xi_{02}) = 10^6 \text{ K}. \quad (4)$$

The parameter  $\xi_{01}$  determines the plasma region with temperature different from the maximum temperature by not more than 10%, and the parameter  $\xi_{02}$  the plasma region with a temperature  $T \geq 10^6$  K. Using the variable  $x$ , we write the expression for the width of the high-temperature plasma region in the form

$$\Delta x = \xi_0 h. \quad (5)$$

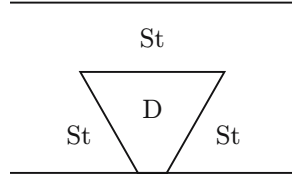


Fig. 6

Fig. 6. Diagram of a steel target (St) with a cavity in the form of a truncated cone filled with deuterium (D).

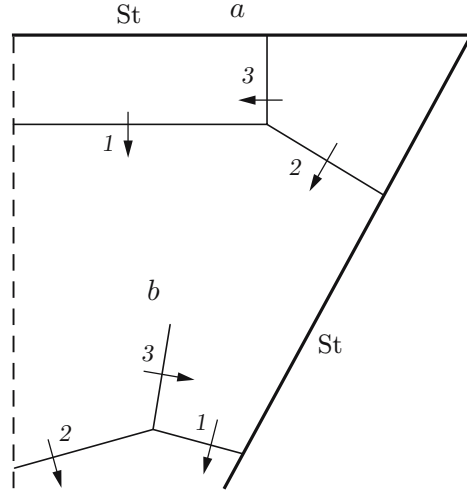


Fig. 7

Fig. 7. Diagram of shock waves in the cone before the reflection (a) and after the reflection (b) from the symmetry axis (dashed line): 1) incident wave; 2) Mach wave; 3) reflected wave; the arrows show the direction of the shock-wave velocity.

The values of the dimensionless parameters  $\tau_0$ ,  $\xi_{01}$ , and  $\xi_{02}$ , given by formulas (2) and (4) for two shock waves and two types of wall are also given in Table 1. The dimensionless time of establishment  $\tau_0$  is almost independent on the type of wall and decreases slightly with increasing  $p_s$ . The smallness of the parameter  $\xi_{01}$  is due to a sharp reduction of the temperature near its maximum (see Fig. 1c). The value of the parameter  $\xi_{02}$  for a shock wave with a pressure  $p_s = 150$  GPa is an order of magnitude larger than the value of the parameter  $\xi_{01}$  and, as might be expected, it decreases considerably with decreasing  $p_s$ . We note that the parameters  $\xi_{01}$  and  $\xi_{02}$  are almost independent on the type of wall.

Using formulas (3) and (5) and the data of Table 1, we calculate the plasma parameters for  $h = 1$  cm and  $p_s = 150$  GPa in the case of a steel plate:  $\Delta t = 0.25 \mu\text{sec}$ , the dimension of the plasma region is  $\Delta x \approx 10 \mu\text{m}$  at  $T \geq 10^6$  K and  $\Delta x \approx 1.7 \mu\text{m}$  at  $T \approx 3 \cdot 10^6$  K.

**3. Shock-Wave Amplification in a Conical Target.** Since the introduction of a strong shock wave into solid deuterium involves difficulties, we consider the problem whose solution indicates that the shock wave in deuterium can be considerably amplified by using conical targets. In a steel target there is a cavity in the form of a truncated cone (the radius of the smaller base of the cone is  $r_0$ , that of the larger base is  $5r_0$ , and the angle between the bases and the lateral surface is  $60^\circ$ ) filled with solid deuterium (Fig. 6). The lower boundary of the target and the lower base of the cone are free boundaries with a pressure  $p = 10^5$  Pa. A shock wave is initiated at the upper base of the cone in the target. We assume that an aluminum impactor (for which the equation of state is given in [6]) collides with the target at a velocity of 10 km/sec. The thickness of the impactor is chosen great enough so that the rarefaction wave from its rear boundary has no time to affect the flow in the cone. Calculations by the equations of state yield a shock-wave pressure in the steel approximately equal to 250 GPa and a pressure of the wave entering deuterium approximately equal to 12 GPa.

In cylindrical coordinates  $(r, z)$ , the vector of the velocity [see Eqs. (1)] is  $\mathbf{u} = (u_r, u_z)$ , and the differentiation operators become  $d/dt = \partial/\partial t + u_r \partial/\partial r + u_z \partial/\partial z$ ,  $\text{div } \mathbf{u} = r^{-1} \partial(r u_r)/\partial r + \partial u_z/\partial z$ , and  $\nabla p = (\partial p/\partial r, \partial p/\partial z)$ . Numerical solution of the problem was performed using the same software package as in the calculations of [8].

Figure 7 shows the system of shock waves (described in [9, 10]) resulting from the entry of a plane shock wave into a cone and the subsequent irregular reflection of the shock waves from the lateral boundary and the symmetry axis. The plane shock wave is first [3] reflected from the lateral boundary in the form of a Mach wave and a reflected wave, which, together with the point of intersection of the three waves, moves to the symmetry axis

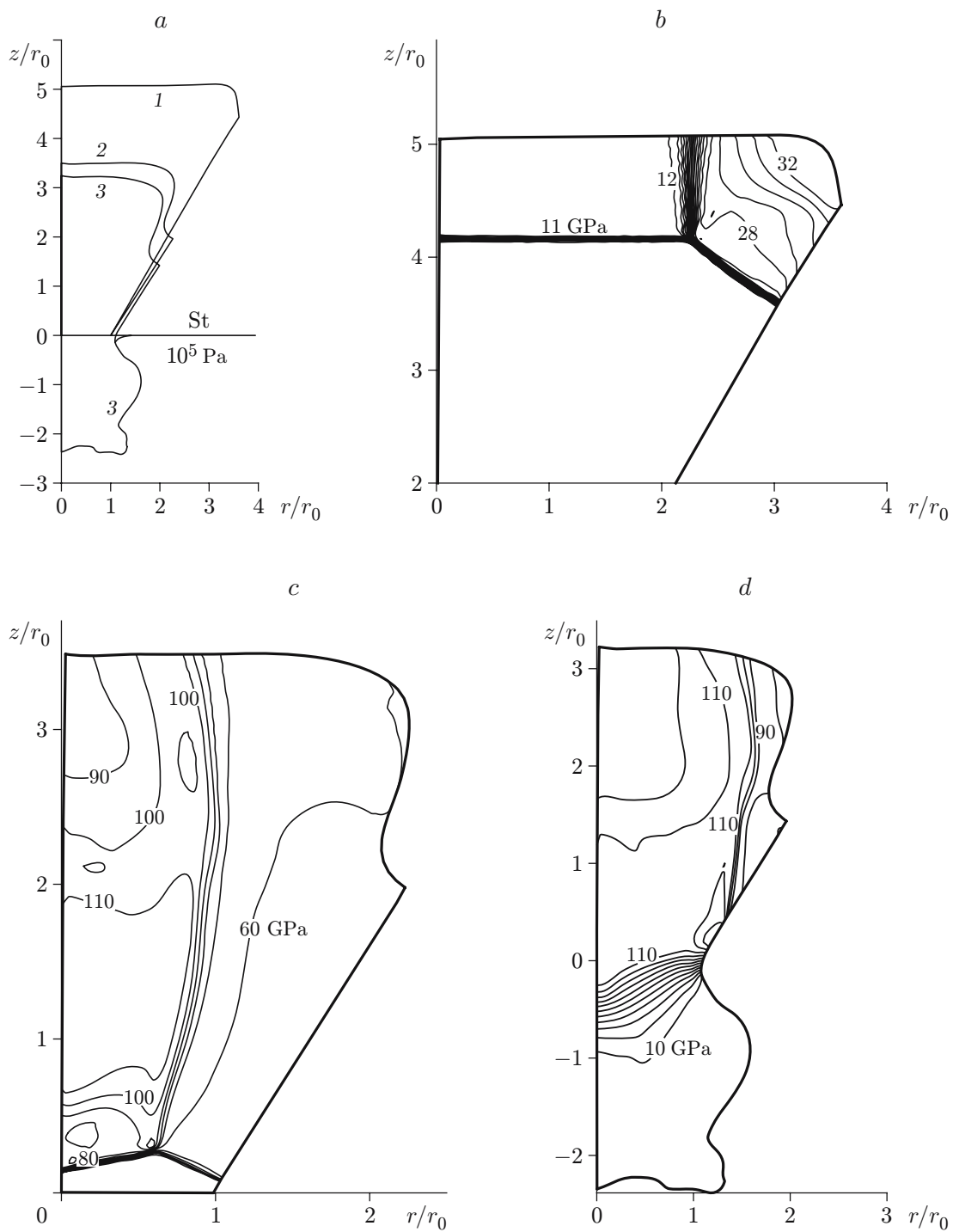


Fig. 8. Boundaries of the deuterium region (a; curves 1, 2, and 3 refer to  $t = t_1$ ,  $t_2$ , and  $t_3$ , respectively) and isobars in deuterium (b-d) at various times:  $t = t_1$  (b),  $t = t_2$  (c), and  $t = t_3$  (d).

(Fig. 7a). When the point of intersection reaches the symmetry axis, the initial plane shock wave disappears and the initial Mach wave begins to be reflected in the form of a new Mach wave and a reflected wave moving from the symmetry axis to the lateral boundary (Fig. 7b).

The results of calculation of the problem are given in Fig. 8, which shows the boundaries of the deuterium volume and the corresponding pressure fields inside it at various times. The curvature of the upper boundary of the deuterium volume near the lateral boundary is due to the occurrence of a cumulative steel jet. Nevertheless, the behavior of shock waves in deuterium agrees with the classical model presented in Fig. 7 since the shock-wave velocities far exceed the cumulative jet velocity. The time shown in Fig. 8b corresponds to the diagram of shock waves in Fig. 7a (the pressure at the front of the initial plane wave is 11.7 GPa, and the pressure behind the reflected wave and the Mach wave is approximately equal to 30 GPa).

Figure 8c shows the time corresponding to the rime corresponding to the beginning of the arrival of shock waves in deuterium at the free boundary when the reflection of the first Mach wave from the symmetry axis has already occurred. The arrangement of the waves and direction of their motion correspond to those shown in Fig. 7b. At the front of the first Mach wave located between the point of intersection of the three waves and the lateral boundary of the cone, the pressure is approximately 50 GPa. At the front of the second Mach wave, located between the point of intersection and the symmetry axis, the pressure is approximately equal to 80 GPa, and inside the target between the symmetry axis and the reflected shock wave, 90–110 GPa.

Figure 8d shows the flow pattern corresponding to the moment after the arrival of the Mach waves at the free surface and the formation of the rarefaction wave. The reflected shock wave is shifted to the lateral boundary, and the pressure field behind it exceeds 100 GPa almost throughout the deuterium volume in the target. As a result, the pressure on the inner boundary of the rarefaction wave is approximately equal to 110 GPa (see Fig. 8d).

**Conclusions.** Shock waves with a pressure  $p_s = 70\text{--}150$  GPa in solid deuterium after the rarefaction and repeated compression on an absolutely solid or steel wall make it possible to produce a plasma [with a particle density of the order of  $10^{22}$  cm $^{-3}$  and a temperature  $(1\text{--}3) \cdot 10^6$  K] in a small region near the wall, in which thermonuclear fusion is possible. In the examined problem, at the same shock intensity the temperature far exceeds the temperature behind the attached shock front under shock compression of deuterium plates on a wedge-shaped target [11].

The dimension of the high-temperature plasma region and the time of its establishment are proportional to the distance between the free surface and the wall. For a shock wave with a pressure of 150 GPa and a steel wall at  $h = 1$  cm, the time of establishment is approximately  $0.25$   $\mu\text{sec}$ , and the dimension of the plasma region at a temperature  $T > 10^6$  K is approximately equal to  $10$   $\mu\text{m}$ .

High-temperature plasma arises in the entropy trace with constant pressure and velocity. Ignoring the possible temperature decrease due to heat transfer and finite cross-sectional dimensions of the gap between deuterium and the wall, the time of existence of the plasma is determined by the difference between the moment the rarefaction waves moving in the relatively cold material from the shock wave generator or from the plate free boundary arrive at the wall and the moment of plasma formation. Under the above assumptions, the time of existence of the high-temperature plasma does not depend on the sound velocity in it, unlike in other methods of plasma generation, in at which a high temperature arises in the region of a high pressure gradient.

Conical solid-state targets may be effective for producing high pressures under shock loading of solid deuterium and, hence, high mass velocities during subsequent unloading. In the examined example, the pressure behind the shock front leaving such a target increases by a factor of 10 times compared to the intensity of the incoming plane shock and reaches  $p_s \approx 100$  GPa.

The temperature distribution in the entropy trace can be affected by heat conduction, which in the present work is not considered. An increase in the distance  $h$  leads to a decrease in the heat conductivity, as follows, in particular, from the energy equation in the variables  $(\tau, \eta)$ , which includes the corresponding term with the multiplier  $h^{-1}$ .

This work was supported by the Russian Foundation for Basic Research (Grant Nos. 07-01-00098 and 06-02-17464) and Program No. 3 of the Department of Mathematical Sciences of the Russian Academy of Sciences.



## REFERENCES

1. Ya. B. Zel'dovich and Yu. P. Raizer, *Physics of Shock Waves and High-Temperature Hydrodynamic Phenomena*, Academic Press, New York (1967).
2. V. Ya. Ternovoi, "Experimental study of thermodynamic and electrically conducting properties of dense media under intense shock-wave loading," Doct. Dissertation in Phys. and Math. Sci., Chernogolovka (2004).
3. K. P. Stanyukovich, *Unsteady Motion of Continuous Media* [in Russian], Gostekhteorizdat, Moscow (1955).
4. V. E. Fortov, K. V. Khishchenko, P. R. Levashov, and I. V. Lomonosov, "Wide-range multi-phase equations of state for metals," *Nucl. Instr. Meth. Phys. Res., A*, **415**, No. 3, 604–608 (1998).
5. M. D. Knudson, D. L. Hanson, J. E. Bailey, et al., "Principal Hugoniot, reverberating wave and mechanical reshock measurements of liquid deuterium to 400 GPa using plate impact techniques," *Phys. Rev. B*, **69**, No. 14, 144209-1–144209-20 (2004).
6. A. V. Bushman, V. E. Fortov, G. I. Kanel', and A. L. Ni, *Intense Dynamic Loading of Condensed Matter*, Taylor and Francis, Washington (1993).
7. Yu. F. Alekseev, L. V. Al'tshuler, and V. P. Krupnikova, "Shock compression of two-component paraffin-tungsten mixtures," *J. Appl. Mech. Tech. Phys.*, No. 4, 624–627 (1971).
8. V. V. Milyavskii, V. E. Fortov, A. A. Frolova, et al., "Calculation of shock compression of porous media in conical solid-state targets with an exit hole," *Zh. Vychisl. Mat. Mat. Phys.*, **46**, No. 5, 913–931 (2006).
9. V. A. Belokon', A. I. Petrukhin, and V. A. Proskuryakov, "Entry of a strong shock wave into a wedge-shaped cavity," *Zh. Éksp. Teoret. Fiz.*, **48**, No. 1, 50–60 (1965).
10. R. E. Setchell, E. Storm, and B. Sturtevant, "An investigation of shock strengthening in a conical convergent channel," *J. Fluid. Mech.*, **56**, No. 3, 505–522 (1972).
11. A. A. Charakhch'yan, "Shock compression of a plate on a wedge-shaped target," *J. Appl. Mech. Tech. Phys.*, **42**, No. 1, 14–20 (2001).